Shielding and Activation Analyses for SNS 200 kW Ring Injection Beam Dump, Title I Design

Irina Popova and Jim Bucholz
Spallation Neutron Source Project
Oak Ridge National Laboratory
701 Scarboro Road, MS-6474
Oak Ridge, Tennessee 37830
(865) 220-5281

ABSTRACT

The Spallation Neutron Source ring injection beam dump has been designed to absorb and stop a 200kW proton beam at 1-GeV. As a part of the Title-I design process, detailed shielding and activation analyses have been performed. The fluxes and dose rates have been calculated on the floor of the operating deck above the beam dump. Activation calculations have been carried out for all materials comprising the beam dump, and for the surrounding soil. The heating rates have been verified in each of 25 copper plates forming the heart of the beam dump.

I. INTRODUCTION

There are three beam dumps associated with the Spallation Neutron Source (SNS): the linac beam dump, the ring injection dump, and the ring extraction dump. The second beam dump is the largest of the three beam dumps and the subject for this paper [1].

Part of the proton beam is lost during injection into accumulator ring and must be safely terminated. Under nominal conditions, approximately 10% of the main (1.0-GeV, 2-milliamp) proton beam may be deflected into this beam dump, thus resulting in the deposition of up to 200 kW of energy in the copper plate assembly comprising the central portion of the beam dump. The copper plate assembly consists of 25 flat copper plates of varying thickness, separated by cooling water, inside a cylindrical steel container. The incident proton beam generates a large number of neutrons and gammas, numerous lightweight particles, and a vast array of residual nuclides that are remnants of the spallation process. All of these generate heat that must be removed, and radiation sources for which shielding must be provided. For shielding purposes, the cylindrical copper plate assembly is surrounded by one-to-two meters of carbon steel on the sides and bottom, and somewhat more in the vertical direction leading to the floor of the operating deck. This massively large steel shield is then surrounded by a thick concrete vault, which provides additional shielding. The concrete vault is below grade and surrounded by soil. Reducing soil activation to acceptable levels may be one of the parameters that may impact the required shield thickness. The dose rate on the floor of the operating deck above the beam dump will be another key consideration. Another objective was to perform activation calculations for all materials comprising beam dump.

II. BASIC CALCULATION MODEL

The MCNPX [2] Monte Carlo code has been used for dose rate estimation on the floor of the operating deck above the beam dump and for the calculation of energy deposition in the copper disks. For activation calculations the newly developed Activation Analysis System [3] (AAS) including the OriHet95 [4] isotope production and depletion module was used. The preliminary step for AAS is a 3-D MCNPX flux calculation, which also tabulates and stores high-energy reaction rates in all materials of interest.

The general 3-D MCNPX model for the ring injection beam dump was based on the detailed SNS engineering drawing [5] and is illustrated in Fig. 1. This model, with a few minor changes, has been used for both the shielding analysis and the activation analysis.

The cylindrical copper plate assembly resides inside a small voided rectangular cavity. Each of the cylindrically-shaped flat copper plates has an outer radius of 15.0 cm, but the thickness of each varies in a non-uniform fashion so as to yield roughly the same amount of energy deposition in each copper plate. The surrounding stainless steel vessel is 1.0 cm thick radially, and on the downstream end, but has a 0.2-cm-thick window on the upstream surface. The total length is 78.6 cm. The rectangular-shaped water-filled region atop the copper plate assembly (Fig. 2) is used to simulate the

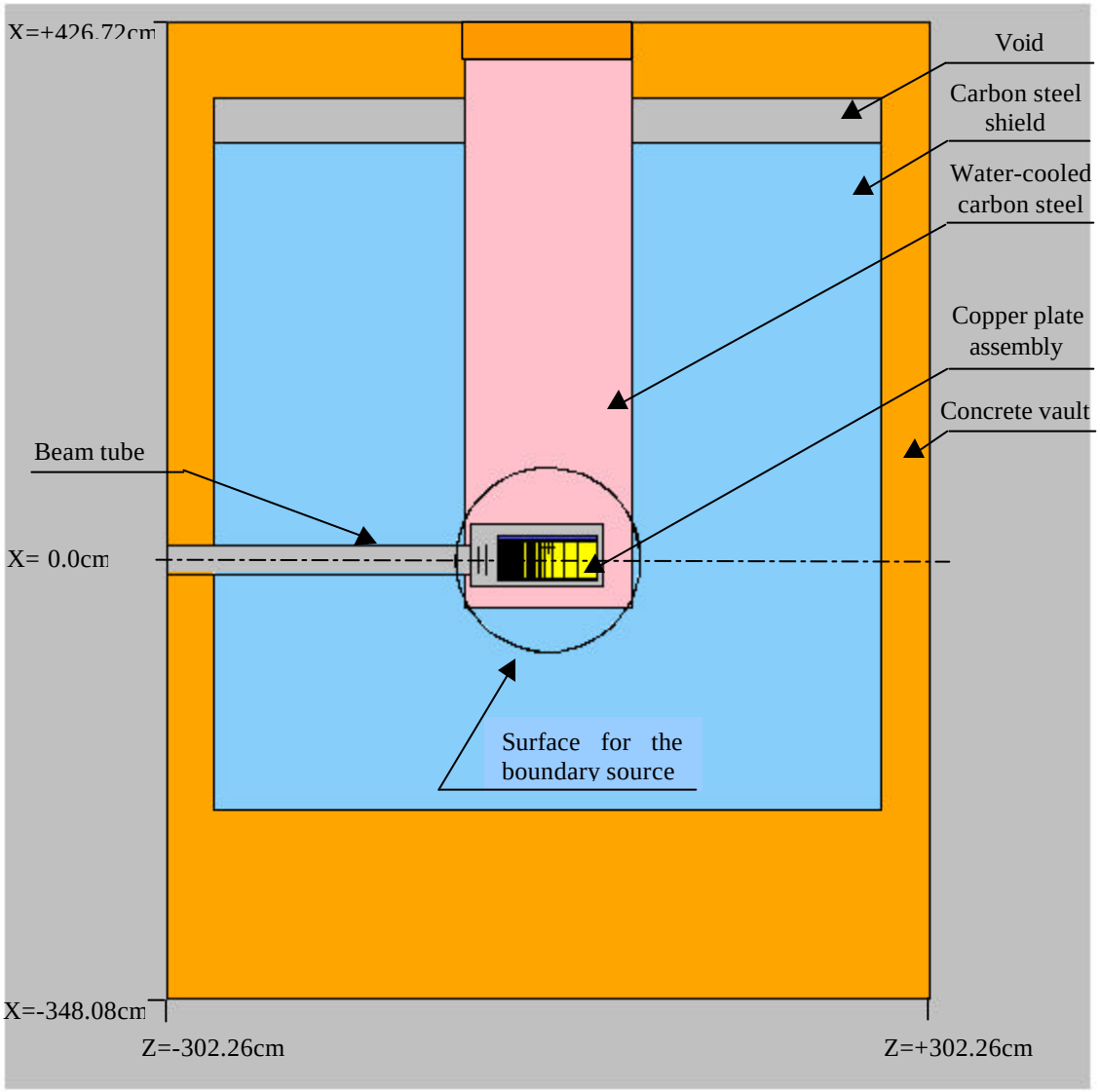

Fig. 1. MCNPX model for the ring injection dump

inlet and outlet cooling lines in approximately this same location. The thick carbon steel shield surrounds the cooper plate assembly. Above most of the carbon steel shield, but below concrete floor of the operating deck, is a 30.48 cm void space. Extending down the center of the bulk steel shield is a removable rectangular-shaped block of water-cooled carbon steel. This is actually comprised of several offset rectangular slabs with a thin tube of water coolant tracing between the steel slabs. This removable portion of the shield is assumed to be 95 vol% carbon steel and 5 vol% water. A thick concrete vault surrounds the carbon steel shield.

At the end of the beam tube, inside the cavity, there is a hemispherical-shaped inconel window represented in the model by three flat disks (inconel, water, and inconel) inside the cavity, downstream of the beam tube but upstream of the copper plate assembly.

The source is specified as a monoenergetic (1000 MeV), monodirectional proton beam (in the +Z direction, pointing into the beam dump) in the basic calculational model. The spatial distribution is a peaked Gaussian distribution in both the vertical (X):

$$S(x) = \exp\left[-\left(\frac{1.6651 * x}{5.0}\right)^2\right] \quad (1)$$

and the horizontal (Y) directions:

$$S(y) = \exp\left[-\left(\frac{1.6651 * y}{2.5}\right)^2\right] \quad (2)$$

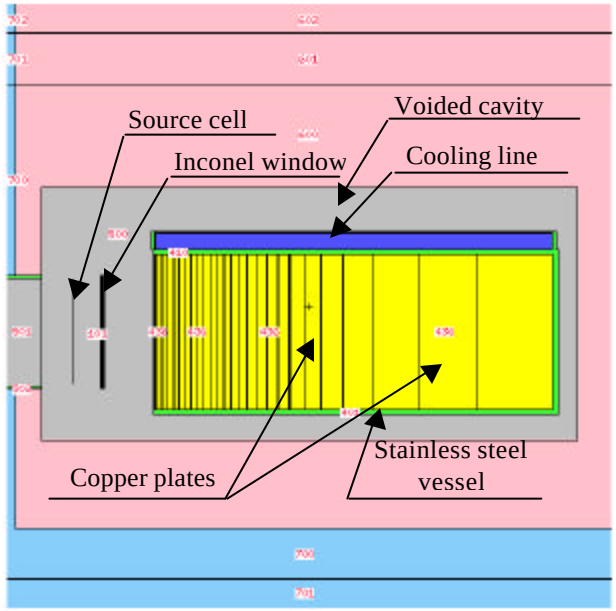

Fig. 2. MCNPX model for copper assembly.

This source is distributed over the finite limits of a 20 cm × 10 cm elliptically-shaped void cell defined upstream of the window inside the voided rectangular cavity. The effect of this cell is to "clip off" or limit the Gaussian distribution in the X and Y directions.

The main portion of the beam diverted into the 200 kW ring injection beam dump is 0.2 mA. Thus, the total number of "protons per second" impinging on the 200 kW ring injection beam dump may be computed as:

$$S_p = (0.0002A) * [(1.0 coul/s)/A] * \left[\frac{1 \cdot proton}{1.602 * 10^{-19} coul}\right] \qquad (3)$$

$$S_p = 1.24844 * 10^{15}\ proton/s$$

This important parameter is specified on the MCNPX tally cards and is used to get the final fluxes and currents in absolute units on n/s/cm2, etc.

Nine different types of particles are physically tracked in the MCNPX Monte Carlo calculations: protons, neutrons, gammas, pi_+ particles, pi_0 particles, deuterons (H-2), tritons (H-3), He-3, and alphas (He-4). Most are generated by spallation events in or near the copper plate assembly.

III. ACTIVATION ANALYSIS

Detailed activation analyses have been performed for all materials comprising the beam dump - i.e., the copper plate assembly, the cooling water, the stainless steel vessel, various subregions of the surrounding carbon steel shield, the concrete vault and the soil.

A. Methods

The activation analyses are performed in two steps. First, the analysis requires knowledge of the residual and gaseous nuclides produced in spallation events by high-energy particles above 20 MeV, as well as conventional nuclide production rates due to neutrons below 20 MeV. This requires use of MCNPX. In this step, the neutron fluxes below 20 MeV are tallied, and data files containing information about every neutron interaction that occurs in the system above 20 MeV are saved in the binary (LAHET [6] type) "histp" file created by MCNPX. The second step involves use of the ORNL Activation Analyses System (AAS) that is shown in Fig. 3. This modular code system includes many different nuclear codes and nuclear data libraries, and combines them with user-generated MCNPX results in such a way as to perform the entire activation analyses in highly automated fashion.

By running the MCNPX "histp" file through the HTAPE3X post-processor code, first with option IOPT=8 and then again with option IOPT=14, HTAPE3X will generate a detailed inventory of the residual nuclide production rates and the light gas (hydrogen and helium) the production rates, by cell, due to neutrons above 20 MeV. The MCNP_RESID command script is used to run the HTAPE3X code. The AAS also contains the MCNP_FLUX command script for reading the low-energy flux tallies (below 20 MeV) produced by MCNPX for every cell of interest. The PARSE_MAT script reads the nuclide-dependent material descriptions from a user's MCNPX input file, while the MCNP_MAT command script runs the GROUPIE code to extract the various FENDL-based particle production-rate cross sections for each nuclide in each material, and tally the resulting light nuclides and heavier residual nuclides that are produced by neutrons below 20 MeV. The MV_DATA command script uses the COMBI code to combine the low-energy

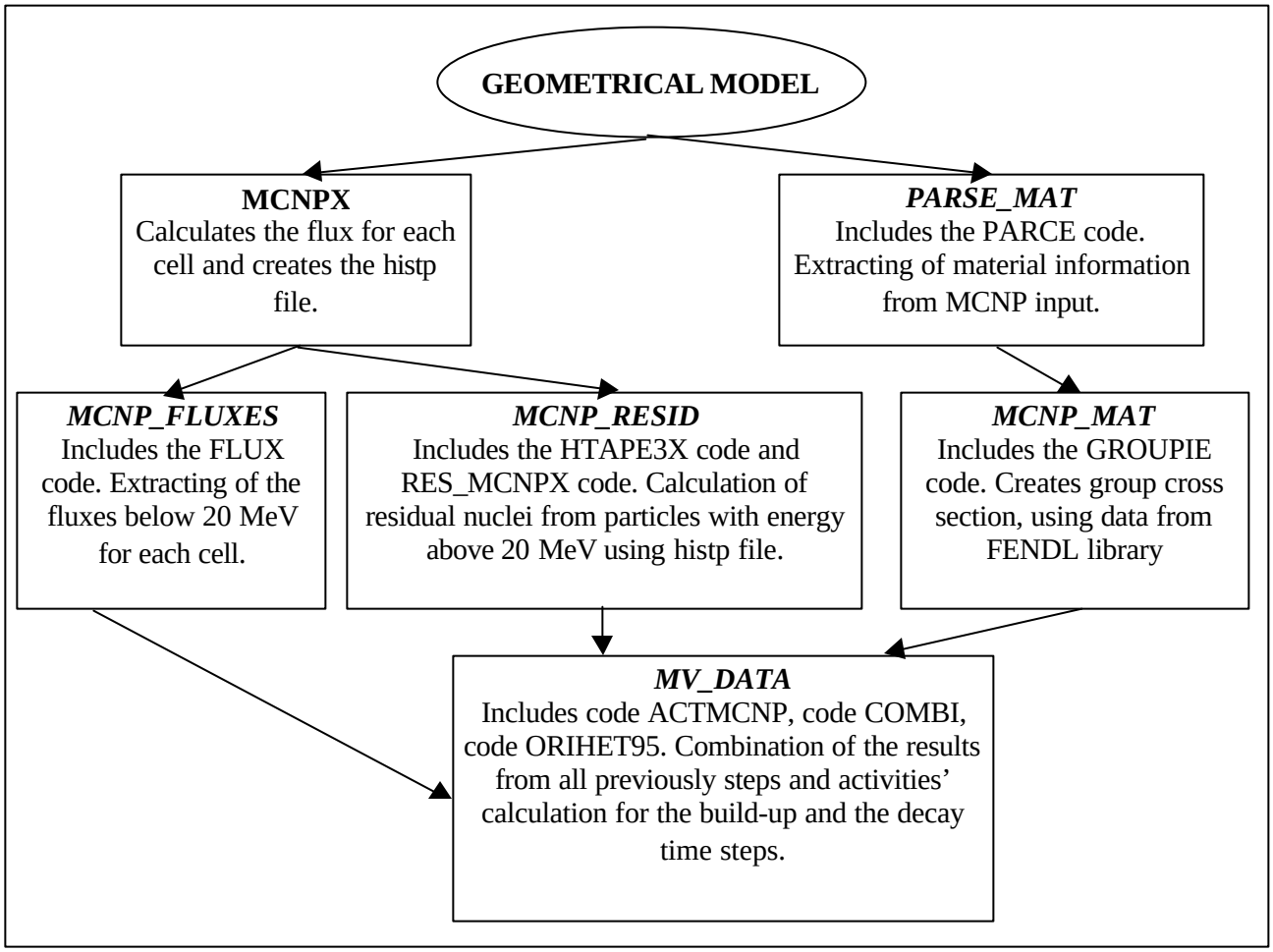

Fig. 3. Activation Analyses System

nuclide production rates with the high-energy production rates from the HTAPE3X post-processor in order to obtain the "total" production rate for a large number of resulting nuclides in each cell. These total production rates are then fed to the OriHet code that is also part of MV_DATA command script. The OriHet code uses these total production rats, as well as internal decay constants, in the final OriHet buildup/decay calculations. This code produces concentration files and other data files (curies, gamma powers, etc) for several hundred nuclides in each cell, at each of 10 timesteps during the irradiation period, and at each of 10 timesteps during the decay period following a specified irradiation time.

B. Soil Activation Analysis

Because it is a deep penetration problem, the MCNPX analysis for soil activation has been divided into two parts for getting results with good statistics. The first part is the determination of an internal boundary source. The second part is final transport calculation using a couple of variance reduction techniques: simple geometric splitting and source energy biasing (for which a multigroup description of the source is necessary).

The internal boundary source has been calculated on an imaginary 73-cm-radius sphere in the bulk steel shield around the copper plate assembly (Fig. 1). To obtain a multigroup description of the source, the following technique has been applied. First, the ssw option in MCNPX was used to save the particles track information (the wssa file) for all type of particles crossing the imaginary 73-cm-radius sphere (Fig. 1). This location was chosen so as to be close enough to the copper plates assembly that we would have good statistics, but far enough away that contribution from everything except

neutron and gammas would be negligible. This boundary source was then processed through the MTA ("MCNP-to-ANISN") coupling code [7] that converts it to multiple ANISN-type “shell sources” [8] including equivalent angular-dependant multigroup sources characteristic of a range of directions specified by the user. Note that the source is not uniform in each direction. Downstream of the beam (+Z), the source less intensive but more energetic than upstream (-Z). The sources in bottom (-X), top (+X) and sides (+Y, -Y) directions are due to leakage from the copper plates, but they are different because the distance from the copper plates to the boundary source sphere in the carbon steel shield is not equal for those directions. The MTA code allows averaging the MCNPX source over some portion of the imaginary source sphere. The equivalent angular-dependent multigroup ANISN sources have been produced for the upstream and downstream sides of the beam dump, as well as the horizontal sides and the bottom portion of the boundary source sphere, while that for each direction has been averaged over that portion of the imaginary source sphere that lies within 45-degrees of the corresponding direction. To make the source description more tractable in MCNPX, the angular distribution of the source in each group was simplified. Separate 1-D (spherical) ANISN calculations have been done for each direction using the angular-dependent multigroup MTA source to obtain the integrated source in each energy group in the first geometry region near the imaginary sphere.

The second part requires a separate 1-D (spherical) MCNPX calculation to be performed for each of the principle directions. Geometric splitting in spatial importance zones spaced roughly 0.15 m apart was also necessary as a variance reduction measure, while fluxes and reaction rates are tallied over the full domain of each spherical shell for better statistics. Lastly, and most importantly, the use of the multigroup MTA source (based on earlier MCNPX calculations) made possible the use of source-energy-biasing which was absolutely essential to obtain adequate statistics. Thus, through a combination of these techniques, the fractional standard deviations in the soil, beyond the 1.6 to 2.6-m-thick steel shield and 0.4-m-thick concrete vault, were reduced to very acceptable levels of 2-3%. Those highly converged fluxes, as well as the high-energy nuclide production rates in the “histp” file, were then used in the subsequent soil activation analyses. These analyses have been performed for the actual isotopic composition of Tennessee soil as measured at the SNS site using spectrographic analyses. This official “reference” sample weighed 1.60904 g/cc and contained a total of $7.43710*10^{-2}$ atoms/(barn*cm).

Exposure periods based on one year and/or 30 years of continuous operation have both been used for the build-up portion of the activation analysis, and as initial conditions for the subsequent decay calculations. The results for 10 of the more important isotopes from the point of view of soil activation are shown in Table 1 after 30 years of operation. The subsequent environmental review concluded that the present shielding design was adequate from the viewpoint of soil activation.

C. Activation Analysis for the Materials Comprising the Beam Dump

The most important area of interest for day-to-day operations, maintenance operations, and for ultimate decontamination and decommissioning, is the central part of the beam dump (i.e., the copper plate assembly, stainless steel vessel, inconel beam tube and cooling water). On a day-to-day basis, one concern is that the tritium generated in the cooling water may find its way to the off-gas system and must be filtered. Also the copper plate assembly forming the core of the beam dump must be periodically removed and replaced. This will be highly activated and will require some sort of storage cask. Moreover, temporary shielding will also have to be designed to protect maintenance workers from radiation coming from the rectangular-shaped water-cooled carbon steel insert that must first be removed to gain access to the copper plate assembly. Gamma source terms resulting from the activation of the copper plate assembly and its stainless steel shell will be used for that. The knowledge of activation levels throughout the bulk steel shielding will ultimately be needed to address issues connected to decontamination and decommissioning near the end of life.

The geometric model used for this analysis was essentially the same as the basic MCNPX model previously described (Fig. 1). The removable rectangular-shaped water-cooled steel region above the copper plate assembly was divided in the +X direction (vertical) into a number of different importance regions. The bulk steel shield was also subdivided into a number of concentric rectangular-shaped importance zones extending outward from the copper plate assembly. These were used for geometrical biasing and for determining the spatial distribution of activation products throughout the water-cooled steel region and the bulk steel shield.

Exposure periods of one year (5000 operating hours) and 30 years of operation have both been used for the build-up portion of the activation analysis, and as initial conditions for the subsequent decay calculations. Decay calculations have been done for one week after shutdown, subsequent to 5000 hours of continuous operation and for one week after shutdown, subsequent to 30 years of continuous operation.

Table 1. Activities in the first 12.7cm soil past concrete wall after 30 years.

Isotope	Concentration, (g-atom)/cm^3			
	Bottom beam dump	Side beam dump	Down stream beam	Upstream beam
H-3	4.70E-15	3.06E-16	1.06E-14	8.81E-16
C-14	8.23E-15	8.51E-15	1.10E-13	1.51E-13
Na-22	1.93E-16	3.77E-18	5.88E-16	7.70E-17
Mn-53	0.00E+00	0.00E+00	0.00E+00	0.00E+00
Mn-54	0.00E+00	0.00E+00	0.00E+00	0.00E+00
B-10	3.34E-15	1.92E-16	1.30E-14	3.62E-16
Al-26	4.30E-15	1.17E-16	8.09E-15	9.87E-16
Cl-36	1.41E-16	2.28E-18	1.22E-16	1.40E-17
K-40	1.08E-14	6.72E-14	7.76E-13	1.20E-12
Ca-41	6.53E-17	2.98E-16	3.45E-15	5.35E-15

The decay gamma heating rates (watts/cc) for the build-up and decay calculations are shown in Table 2 for the copper plates, stainless steel vessel, cooling water and water-cooled rectangular carbon steel region adjacent to the voided rectangular cavity, and the edge of the bulk steel shield closest to voided cavity (outside water-cooled region). The tritium concentrations (g-atom/cm^3) are also presented for these same regions.

In particular, it should be noted that, after one accounts for the relative volumes, 26.7 times more tritium would be generated in the copper plate assembly than in the surrounding cooling water after 30 years of operation. In and around the copper plate assembly, the production of tritium by high-energy reactions above 20 MeV is one to two orders of magnitude more important than the production of tritium by low-energy reactions below 20 MeV. Low-energy neutrons below 20 MeV, for example, account for only 1.2% of the tritium produced in the copper, 4.5% of the tritium produced in the surrounding stainless steel shell, and only 11.1% of the tritium produced in the water. As a result of these findings, the ORNL Activation Analysis System (AAS) was augmented in April 2000 to automatically account for the high-energy gas production terms above 20 MeV. It is also interesting to note that the amount of tritium produced in some materials may be 1000 to 2000 times higher than what one would estimate with standard ORIGEN [9] libraries based on thermal neutron capture in hydrogen and deuterium. Much of this "extra" production was due to (n,t) reaction-rate thresholds that exist in many materials between 5 and 12 MeV, and a second threshold that may exist in some materials between 14 and 15 MeV.

Table 2. The decay gamma heating rates (watts/cc) and the tritium concentration (g-atom/cm^3) for copper plates, stainless steel vessel, cooling water and edge of water-cooled rectangular carbon steel region, and the edge of the bulk steel shield immediately after voided rectangular cavity.

Locations		Copper plates	Stainless steel vessel	Cooling water	Water-cooled carbon steel	Bulk carbon steel shield
Gamma heating rates	5000 hours	3.13E-03	1.01E-02	4.02E-05	9.72E-05	1.93E-05
	1 week decay	1.04E-03	4.95E-04	4.68E-07	5.19E-05	9.85E-06
	30 year	4.05E-03	1.03E-02	4.02E-05	1.27E-04	2.61E-05
	1 week decay	1.97E-03	6.98E-04	5.01E-07	8.15E-05	1.64E-05
Tritium	5000 hours	5.81E-08	6.19E-09	1.08E-08	3.66E-10	1.45E-11
	30 year	1.50E-06	1.60E-07	2.78E-07	9.42E-09	3.74E-10

IV. DOSE RATE AND FLUX CALCULATIONS

Dose rates and fluxes on the operating floor above the beam dump have been determined. Because this was a deep penetration problem, the task was divided in two parts for getting results with good statistics. As before, the first part was the determination of the internal boundary source ("wssa" file) on an imaginary 73-cm-radius sphere in the bulk steel shield around the copper plate assembly. Then the MTA code was used to

determine the equivalent multigroup source over that portion of the imaginary source sphere that lies within 45 degrees of the +X axis extending from the copper plate assembly to the operating deck above the beam dump.

The initial shielding calculations used the ANISN code with HILO88 multigroup library [10] for the second part of this analysis. Unfortunately, that cross section library was found to underestimate the low-energy fluxes (below 1.1 MeV) deep in the shield. Comparisons of ANISN results against MCNPX results showed that the use of ANISN with the HILO88 library severely underestimates thermal neutrons and secondary gammas deep in the shield, sometimes by as much as two orders of magnitude.

To avoid this problem, the MCNPX code was ultimately used instead. The technique described in Section III part B that allows source energy biasing was again applied, except that now a full 3-D model has been used in the second part of shielding analysis. In order to obtain credible results in a reasonable amount of computer time, source-energy biasing and extensive use of simple geometric splitting were both absolutely essential.

The neutron and gamma dose rates have been tallied in the radial direction atop the floor of the operating deck, and are presented in Table 3. These results clearly reveal that the total dose rate peaks at about 8.3 mrem/hr, not at the centerline, but at a location about 100 cm from the centerline. This 3-D effect is caused by the fact that the removable water-cooled steel region extends all the way up to the concrete floor plug, while above the nearby bulk steel shield there is a 30.48 cm thick void between the bulk steel shield and the concrete floor.

The acceptable dose level is nominally 0.25 mrem/hr. The results show us that the originally planned shielding in this general area was insufficient, with the maximum dose rate of 8.3 mrem/h peaking 1.0 m from the centerline. Additional shielding will have to be provided in the final design to prevent the off center peaking, and a follow-up 3-D shielding analysis will be required.

V. HEATING RATES IN THE COPPER PLATES

Originally, the thickness of the copper plates were optimized so as to obtain a more-or-less uniform heating rate of 5000 watts in all but the last two copper plates. Unfortunately, those earlier optimization calculations only accounted for the transport of protons, neutrons, and gammas. In the present MCNPX calculation we also track pi_+ and pi_0 particles, deuterons (H-2), tritons (H-3), He-3, and alpha particles, which are produced by spallation reactions in the copper plates. The geometric model used for this analysis was the same as the basic MCNPX model previously described in Section II except that each copper plate was designated as a different cell so that the axial distribution of the overall heating rate could be obtained. The +F6 tally was used to determine the aggregate heating rate due to all types of particles.

All results were obtained with good statistics. The fractional standard deviations (fsd) associated with the local heating rates were all less than 1%. Nevertheless, the heating rate in the first copper plate in the assembly was found to be 23% greater than when these special particles had not been explicitly tracked. The plates further downstream were within 2 to 4% of the original values. Fortunately, even the higher heating rates in copper plates are still acceptable and no changes in the design were necessary.

Table 3. Neutron and gamma dose rates radially atop the floor of the operating deck

Radius*, cm	Neutron dose rate, mrem/hr	Gamma dose rate, mrem/hr	Total	Radius, cm	Neutron dose rate, mrem/hr	Gamma dose rate, mrem/hr	Total
39.8	1.8100	0.397	2.207	132.3	5.224	1.914	7.138
56.4	3.855	0.890	4.745	138.2	4.998	1.937	6.935
69.1	3.966	1.230	5.196	143.8	4.607	1.958	6.565
79.7	5.679	1.715	7.394	149.3	3.938	1.746	5.684
89.2	5.978	2.010	7.988	154.5	3.081	1.633	4.714
97.7	6.256	2.071	8.328	159.6	3.229	1.637	4.866
105.6	5.426	2.341	7.767	164.5	3.853	1.871	5.724
112.8	6.341	1.953	8.294	169.3	2.564	1.681	4.245
119.6	4.775	2.135	6.910	173.9	2.998	1.489	4.487
126.1	4.812	2.146	6.958	178.4	3.653	1.453	5.106

*Outer radius of tallied area.

VI. CONCLUSION

Detailed shielding and activation analyses have been performed for the ring injection beam dump with a maximum incident beam power of 200 kW. The fluxes and high-energy reaction rates in the soil, and the dose rates on the operating floor above the beam dump, have been calculated. Both calculations have been performed using a two-step procedure involving the determination of an internal boundary source in multigroup format, followed by 3-D or 1-D MCNPX transport calculations using source-energy-biasing and geometry splitting. Activation analyses for all materials comprising the beam dump and for the surrounding soil have been done. The newly developed ORNL Activation Analysis System, including the OriHet95 isotope production and depletion code, has been implemented and used in all activation calculations.

The review of soil activities shows that the steel and concrete shielding on the sides of the beam dump and below it were judged to be adequate from the viewpoint of soil activation. Decay gamma source terms from detailed activation analyses for all the materials comprising the beam dump will be used for design of temporary shielding required for maintenance operations and for ultimate decontamination and decommissioning. Gamma source terms resulting from the activation of the copper plate assembly and its stainless steel shell after one year and 30 years of operation will be used in scoping calculations for the design of a cask to hold the assembly after periodic replacement.

The analysis of dose rates on the floor of the operating deck shows that they are not presently within acceptable limits and that the biggest concern is the dose rate approximately one meter from the centerline. In the Title-II design, additional steel shielding will be provided to minimize this problem. In the final analysis, a follow-up 3-D shielding analysis will be performed.

Verification calculations for the heating rates in the copper plates have been done. Accounting of all particles produced by spallation reactions will increase the estimated heating rates by 23% in first cooper plate and by 2% in the last one.

REFERENCES

1. J. A. Bucholz, I.I. Popova, “Shielding and Activation Analyses for the SNS 200 kW Ring Injection Beam Dump,” ORNL/SNS (Aug. 15, 2000).
2. L. S. Waters, ed., “MCNPX User’s Manual–Version 2.1.5,” Los Alamos National Laboratory, NM, TPO-E83-G-UG-X-00001 (Nov. 1999).
3. G.S. McNeilly, “Activation Analysis System,” private communication, ORNL (Feb. 2000).
4. F. Atchison, “OriHet95 for the VAX,” ORNL, internal documentation (1984).
5. SNS engineering drawing, M3E087000k001, ORNL (July 1999).
6. R. E. Prael, H. Lichtenstein, “Users Guide to LCS: The LAHET Code System,” LA-UR-89-3014, Los Alamos National Laboratory (Sept. 1989).
7. F. X. Gallimeier, R. E. Pevey, “Creation of Set of Interface Utilities to Allow Coupled Monte Carlo/Discrete ordinates Shielding Analysis,” Proceedings of Third International Topical Meeting on Nuclear Applications of Accelerator Technology, pp.404-409, ANS, Long Beach, CA (Nov. 1999).
8. W. W. Engle, Jr., “A Users Manual for ANISN: A One-Dimensional Discrete Ordinates Transport Code with Anisotropic Scattering,” K-1693, Oak Ridge Gaseous Diffusion Plant, Union Carbide Corp. (March 1967).
9. W. Hermann and R. M. Westfall, “ORIGIN-S: SCALE System Module to Calculate Fuel Depletion, Actinide Transmutation, Fission Product Buildup and Decay, and Associated Radiation Source Terms,” as contained in Vol. 2, Sect. F7 of “SCALE: A Modular Code System for Performing Standardized Computer Analyses for Licensing Evaluation,” ORNL/NUREG/CSD-2/V2/R5 (March 1997).
10. R. A. Lillie, “HILO88 Multigroup Library,” private communication, ORNL (Feb. 2000).